



**HAL**  
open science

## Small-RNA-mediated transgenerational silencing of histone genes impairs fertility in piRNA mutants

Giorgia Barucci, Eric Cornes, Meetal Singh, Blaise Maxime Li, Martino Ugolini, Aleksei Samolygo, Céline Didier, Florent Dingli, Damarys Loew, Piergiuseppe Quarato, et al.

### ► To cite this version:

Giorgia Barucci, Eric Cornes, Meetal Singh, Blaise Maxime Li, Martino Ugolini, et al.. Small-RNA-mediated transgenerational silencing of histone genes impairs fertility in piRNA mutants. *Nature Cell Biology*, 2020, 22 (2), pp.235-245. 10.1038/s41556-020-0462-7. hal-02617478

**HAL Id: hal-02617478**

**<https://hal.science/hal-02617478>**

Submitted on 26 May 2020

**HAL** is a multi-disciplinary open access archive for the deposit and dissemination of scientific research documents, whether they are published or not. The documents may come from teaching and research institutions in France or abroad, or from public or private research centers.

L'archive ouverte pluridisciplinaire **HAL**, est destinée au dépôt et à la diffusion de documents scientifiques de niveau recherche, publiés ou non, émanant des établissements d'enseignement et de recherche français ou étrangers, des laboratoires publics ou privés.

## **TITLE**

**Small-RNA-mediated transgenerational silencing of histone genes impairs fertility in piRNA mutants**

## **AUTHORS**

Giorgia Barucci<sup>1,2,7</sup>, Eric Cornes<sup>1,7</sup>, Meetal Singh<sup>1,7</sup>, Blaise Li<sup>3</sup>, Martino Ugolini<sup>1,4</sup>, Aleksei Samolygo<sup>1,5</sup>, Celine Didier<sup>1</sup>, Florent Dingli<sup>6</sup>, Damarys Loew<sup>6</sup>, Piergiuseppe Quarato<sup>1,2</sup>, Germano Cecere<sup>1,†</sup>

## **AFFILIATION**

<sup>1</sup>Mechanisms of Epigenetic Inheritance, Department of Developmental and Stem Cell Biology, Institut Pasteur, UMR3738, CNRS, Paris, 75015 France

<sup>2</sup>Sorbonne Université, Collège doctoral, F-75005 Paris, France

<sup>3</sup>Bioinformatics and Biostatistics Hub – C3BI, Institut Pasteur, USR 3756, CNRS, Paris, 75015 France

<sup>4</sup>Scuola Normale Superiore, Pisa, Italy

<sup>5</sup>Moscow Institute of Physics and Technology, Moscow, Russia

<sup>6</sup>Institut Curie, PSL Research University, Centre de Recherche, Laboratoire de Spectrométrie de Masse Protéomique, Paris, France

<sup>7</sup>These authors contributed equally

<sup>†</sup>Corresponding author. email: [germano.cecere@pasteur.fr](mailto:germano.cecere@pasteur.fr)

## **ABSTRACT**

PIWI-interacting RNAs (piRNAs) promote fertility in many animals. Yet, whether this is due to their conserved role in repressing repetitive elements (REs) remains unclear. Here, we show that the progressive loss of fertility in *Caenorhabditis elegans* lacking piRNAs is not caused by derepression of REs or other piRNA targets, but rather mediated by the epigenetic silencing of all the replicative histone genes. In the absence of piRNAs, downstream components of the piRNA pathway relocate from germ granules and piRNA targets to histone mRNAs to synthesize antisense small RNAs (sRNAs) and induce transgenerational silencing. Removal of the downstream components of the piRNA pathway restores histone mRNA expression and fertility in piRNA mutants, and the inheritance of histone sRNAs in wild-type worms adversely affects their fertility for multiple generations. We conclude that the sRNA-mediated silencing of histone genes impairs fertility of piRNA mutants and may serve to maintain piRNAs across evolution.

## MAIN TEXT

Among different classes of endogenous small RNAs in animals, PIWI-interacting RNAs (piRNAs) play a conserved role in repressing transposons and other repetitive elements (REs)<sup>1</sup>, and in several animal species the loss of piRNAs causes sterility<sup>2</sup>. Because of the role of piRNAs in transposon silencing, the sterility phenotype observed in animal lacking piRNAs is commonly believed to be caused by derepression of REs and consequently DNA damage<sup>3</sup>. However, non-transposon derived piRNAs promote fertility in mouse<sup>4</sup>, and a piRNA-independent function of one of the PIWI proteins, MIWI, has been implicated in male fertility<sup>5</sup>. Therefore, the requirement of piRNAs and PIWI for animal fertility can be uncoupled from their role in transposon silencing and might be due to additional piRNA regulatory functions. In *C. elegans*, mutations in components of the piRNA pathway show progressive loss of fertility across generations, which ultimately leads to a sterile population of worms<sup>6</sup>. This transgenerational phenotype is often temperature dependent and reversible whereby animals gradually become sterile at elevated temperature and recover their fertility when grown at lower temperature<sup>7–10</sup>. Thus, whether the role of piRNAs in promoting fertility depends on the silencing of REs or other epigenetic mechanisms remains a matter of debate<sup>11</sup>.

The majority of *C. elegans* piRNAs are independently transcribed in the germline from thousands of genomic loci and do not have sequence complementarity to REs<sup>12–16</sup>. However, they regulate their targets even by imperfect complementarity<sup>17,18</sup>. Thus, any REs or other germline-expressed RNA sequences, including protein-coding transcripts are potential targets and their regulation can also contribute to promote fertility. *C. elegans* piRNAs do not directly silence the expression of their targets, but trigger the accumulation of small single-stranded antisense 22G-RNAs, which are loaded into Worm-specific Argonaute proteins (WAGOs). These constitute the downstream effector factors of the piRNA-induced silencing pathway and silence the

complementary targets at the transcriptional and the post-transcriptional levels<sup>8,19,20</sup>. PIWI and its downstream effectors localize to specific perinuclear compartment called germ granules, and some of the structural components of germ granules also participate in heritable RNAi<sup>21–23</sup>.

Here, we investigate the mechanisms underlying the transgenerational loss of fertility in population of *C. elegans* lacking piRNAs. We show that the removal of piRNAs is not sufficient to derepress protein-coding and RE transcripts targeted by the piRNA pathway. Instead, we found that in the absence of piRNAs, the downstream effectors of piRNA-induced silencing complex relocate from piRNA targets to histone mRNAs. This process leads to the accumulation of 22G-RNAs antisense to all the replicative histone genes and to the transgenerational silencing of histone mRNAs, which ultimately lead to sterile animals.

## RESULTS

### piRNA targets are not desilenced in *piwi* mutant

To understand the reduced fertility and transgenerational sterility observed in piRNA mutants<sup>6,12,14</sup>, we identified transcripts directly regulated by piRNAs. We combined small RNA sequencing (sRNA-seq) with strand-specific RNA sequencing (RNA-seq) and compared mutants of the *C. elegans* PIWI protein PRG-1 with wild-type worms, using populations of synchronized young adult worms of the null allele *prg-1(n4357)*<sup>14</sup> almost sterile at 20 °C (Extended Data Fig. 1a). To identify piRNA-dependent 22G-RNA protein-coding targets, we selected 1017 protein-coding genes from which substantially reduced levels of 22G-RNAs were produced (< 4-fold) in the *prg-1(n4357)* mutant compared to wild-type worms. Only 6% (67 genes) of these mRNA transcripts became up-regulated (> 2-fold; *padj* < 0.05) (Fig. 1a). Analysis of 958 RE families revealed that 154 REs had reduced 22G-RNAs (< 2-fold) in *prg-1(n4357)* compared to wild-type worms, yet only three RE families were significantly up-regulated (> 2-fold; *padj* < 0.05) (Fig. 1b).

We also used uniquely mapped reads to analyze the expression of approximately 60,000 discrete REs<sup>24</sup>, and found that less than 100 individual REs were significantly up-regulated ( $\geq 2$ -fold and  $p_{adj} < 0.05$ ) in *piwi* mutant compared to wild-type worms (Extended Data Fig. 1b, d). Therefore, the decrease in 22G-RNAs antisense to protein-coding genes or REs was not sufficient to derepress them, and they were likely kept repressed by nuclear RNAi and/or chromatin factors<sup>24–26</sup>. Indeed, RNA-seq analysis and RT-qPCR of individual REs in the mutant of the nuclear Argonaute HRDE-1, a downstream effector of the piRNA pathway that acts at the transcriptional level, resulted in a larger number of up-regulated REs compared to *prg-1(n4357)* mutant (Extended Data Fig. 1b, d). Nonetheless, the *hrde-1 (tm1200)* mutant analyzed was not sterile and showed only a mild reduced fertility compared to wild-type worms (Extended Data Fig. 1a), suggesting that the derepression of REs might not be correlated with the piRNA mutant phenotype. These results also suggest that piRNAs might only be required to initiate, and not to maintain, the silencing of their targets as proposed by previous research<sup>19,27–29</sup>.

### **Histone mRNA silencing correlates with transgenerational sterility in *piwi* mutant**

The RNA-seq and sRNA-seq analyses also revealed several protein-coding genes that showed reduced mRNA levels and increased 22G-RNAs in *prg-1(n4357)* compared to wild-type worms (Fig. 1a), suggesting they had been silenced by small RNAs. The majority of these transcripts corresponded to the replicative histone mRNAs (Fig. 1a), and most of the histone gene clusters acquired a substantial number of 22G-RNAs causing their complementary mRNAs to become substantially down-regulated (Fig. 1c). We also analyzed by RT-qPCR mRNA levels in the mutant of the piRNA biogenesis factor PRDE-1<sup>30</sup>, and observed a substantial depletion of histone mRNAs (Extended Data Fig. 1c). Mutants of the nuclear Argonaute HRDE-1 did not silence histone mRNAs (Extended Data Fig. 1c, e) and nascent RNA sequencing (nRNA-seq)

revealed only a mild down-regulation of some histone genes in *prg-1(n4357)* compared to wild-type (Extended Data Fig. 1f, g), indicating that the down-regulation of the histone genes occurred at the post-transcriptional level in piRNA mutants.

In *C. elegans*, histone mRNA silencing using RNA interference (RNAi) is sufficient to cause sterility<sup>31,32</sup>. We, therefore, tested whether histone mRNA silencing correlated with piRNA mutant transgenerational loss of fertility. We generated a CRISPR-Cas9 null allele of the PIWI protein PRG-1 (Fig. 1d), selected two independently-edited CRISPR-Cas9 lines and propagated isogenic populations of homozygote *piwi* mutant and wild-type worms (Extended Data Fig. 2b). We maintained these lines for 10 generations until the *piwi* mutant became almost completely sterile (Fig. 1e and Extended Data Fig. 2a), sampling the populations using RNA-seq and sRNA-seq. Mutant worms propagated for two generations after homozygosis (F4) showed no phenotypic differences compared to wild-type worms (Fig. 1e and Extended Data Fig. 2a) and RNA-seq analysis showed very few gene expression changes (Extended Data Fig. 2c). At later generations, individuals from the *piwi* mutant isogenic population started to display fertility defects, including full sterility in some individuals, until the population became almost completely sterile after 10 generations (Fig. 1e and Extended Data Fig. 2a). These results correlated with substantial gene expression changes across generations (Extended Data Fig. 2c-e). The progressive loss of fertility was accompanied by a gradual reduction of histone mRNA transcripts and a gain of 22G-RNAs antisense to histone mRNAs (Fig. 1f and Extended Data Fig. 2f). The modest desilencing of piRNA-dependent 22G-RNA protein-coding and RE targets did not correlate with the progressive loss of fertility (Extended Data Fig. 2f-h). To evaluate the impact of histone mRNA silencing on histone protein levels in germ cells, we generated a CRISPR-Cas9 null allele of PIWI in a transgenic strain expressing a single-copy of histone H2B::mCherry in the germline. Live imaging of wild-type worms confirmed that the H2B::mCherry was normally expressed in the germline and

incorporated into chromosomes (Fig. 1g, Extended Data Fig. 2j). However, *piwi* mutants showed significantly reduced levels of H2B::mCherry in germline nuclei of animals with reduced fertility (Fig. 1g and Extended Data Fig. 2i). Western blotting analysis confirmed the reduced levels of H2B::mCherry in populations of *piwi* mutant worms (Extended Data Fig. 2j), and Chromatin Immunoprecipitation (ChIP) experiments revealed reduced incorporation of H2B::mCherry into the chromatin of *piwi* mutant animals (Fig. 1h). These results are in accordance with the observed defect in chromosome compaction in pachytene nuclei of sterile *piwi* mutant animals (Extended Data Fig. 2k), which can be a consequence of the lack of histone incorporation into chromatin. Altogether, these results suggest that the transgenerational silencing of histone mRNAs, and not the desilencing of piRNA targets, correlates with the progressive loss of fertility observed in *piwi* mutants.

### **The downstream component of the PIWI pathway, WAGO-1, targets histone mRNAs for silencing**

To identify RNAi factors involved in histone mRNA silencing we asked whether Argonaute proteins downstream of PIWI in the piRNA-induced silencing pathway might ectopically load small RNAs derived from histone mRNA transcripts. We identified several Argonaute proteins interacting with PIWI by mass spectrometry, among which many are known to participate in piRNA-induced silencing<sup>20</sup> (Fig. 2a and Supplementary Table 1). The most highly enriched PIWI-interacting Argonaute protein was WAGO-1, which plays a role in the post-transcriptional silencing of piRNA targets<sup>19,33</sup>. We generated a FLAG tagged version of WAGO-1 and confirmed the interaction between WAGO-1 and PIWI by mass spectrometry and Co-immunoprecipitation (Co-IP) experiments (Fig. 2c, and Extended Data Fig. 4a). Next, we immunoprecipitated WAGO-1 associated 22G-RNAs in wild-type and *piwi* mutant backgrounds. In the wild-type background

WAGO-1 was loaded with 22G-RNAs derived from piRNA-dependent protein-coding targets (Fig. 2d), and was not enriched in 22G-RNAs from histone mRNAs (Fig. 2d). In the *piwi* mutant WAGO-1 was instead enriched in histone 22G-RNAs, and the loading of 22G-RNAs derived from piRNA-dependent 22G-RNA targets was significantly decreased (Fig. 2d). Furthermore, in *piwi* mutant worms, WAGO-1 decreases its interaction with mRNAs from piRNA-dependent 22G-RNA targets and instead binds to histone mRNAs (Extended Data Fig. 3a). These results indicate that WAGO-1 relocated from piRNA-dependent targets to histone mRNAs in a 22G-RNA-dependent manner, suggesting that WAGO-1 is one of the Argonaute proteins that promotes histone mRNA silencing in piRNA mutant worms.

### **WAGO-1 gradually loses interaction with germ granule components upon *piwi* mutation**

The quantification by mass spectrometry of PIWI-interacting proteins revealed, in addition to Argonaute proteins and 22G-RNA biogenesis factors, the enrichment of specific germ granule components, which are also known to participate in heritable RNAi<sup>21–23</sup> (Fig. 2a-c, and Supplementary Table 1). WAGO-1 also interacts with some germ granule factors, and preferentially with DEPS-1 (Fig 2b, c, and Extended Fig. 4a), a germ granule component known to participate in RNAi<sup>34</sup>. Many of these factors act downstream of the piRNAs to promote RNA silencing across generations<sup>8,19,20,22,23</sup>. Therefore, PIWI and piRNAs might help to initiate the formation of the piRNA-induced silencing complex in germ granules. To study whether the interactions between the downstream components of the piRNA-induced silencing complex are perturbed upon removal of PIWI proteins, we quantified WAGO-1-interacting proteins by mass spectrometry in wild-type compared to three progressive generations of *piwi* mutants. Our analysis revealed that the interactions between WAGO-1 and germ granule components gradually diminished across generations in absence of PIWI protein (Fig. 3a, b). Instead, WAGO-1

interaction with some Argonaute protein, such as PPW-1 and the WAGO-1-interacting 22G-RNA biogenesis factor RDE-12<sup>35</sup>, was maintained even in late generation of *piwi* mutants (Fig. 3a, b). Taking together, these results suggest that the loss of interaction between WAGO-1 and germ granule components might affect WAGO-1 localization. To test this hypothesis, we performed live imaging of WAGO-1 and the germ granule component PGL-1 in wild-type and *piwi* mutant. Live imaging of a CRISPR-Cas9 strain expressing WAGO-1::GFP in wild-type worms confirmed its predominant perinuclear germ granule localization (Fig. 3c), as previously observed<sup>33</sup>. However, in late generations of *piwi* mutant, WAGO-1 lost its germ granule localization and remained mainly cytoplasmic (Fig. 3c). We confirmed this results by immunostaining experiments using CRISPR-Cas9 WAGO-1::FLAG strain in wild-type and *piwi* mutant worms (Extended Data Fig. 3b). Live imaging of the germ granule component PGL-1 in *piwi* mutant showed that the loss of WAGO-1 germ granule localization was not caused by a disruption of germ granule assembly (Fig. 3c), since PGL-1 granules were still formed even in sterile animals (Extended Data Fig. 3c). In addition, live imaging of the Argonaute protein CSR-1, which does not belong to the piRNA pathway, showed germ granule and cytoplasmic localization in wild-type and *piwi* mutant worms, indicating that the loss of germ granule localization in *piwi* mutant is specific to the WAGO-1 Argonaute (Figure 3c and Extended Data Fig. 3c).

### **The CSR-1 pathway triggers the biogenesis of histone 22G-RNAs**

The data presented so far suggest that in absence of PIWI, another RNAi pathway is responsible to trigger the biogenesis and loading of histone 22G-RNAs into WAGOs. The proteomic analysis of PIWI-interacting proteins revealed the interaction with the Argonaute CSR-1 (Fig. 2a and Supplementary Table 1), which is known to counteract piRNA-silencing on mRNAs<sup>36,37</sup> and to promote histone biogenesis<sup>38</sup>. We confirmed this interaction by Co-IP

experiments using a FLAG tagged CRISPR-Cas9 strain of CSR-1 (Extended Data Fig. 4a). We also analyzed CSR-1-interacting proteins by mass spectrometry and found, in addition to known components of the CSR-1 pathway, interactions with PIWI and WAGO-1 and many of their RNAi- and germ granule-interacting proteins (Fig. 4a, Extended Data Fig. 4d, and Supplementary Table 1). However, some germ granule components, such as DEPS-1, appear to specifically interact only with PIWI and WAGO-1 (Fig. 4a, Extended Data Fig. 4a, b). Nonetheless, the piRNA and the CSR-1 pathways shared many interactors (Fig. 4a), including WAGO-1, and in absence of PIWI, WAGO-1 might preferentially interact with CSR-1 in the cytoplasm. To confirm this hypothesis, we performed Co-IP experiments that show interaction between WAGO-1 and CSR-1 also in *piwi* mutant (Fig. 4b and Extended Data Fig. 4e), even though these mutant animals have lost WAGO-1 germ granule localization and have reduced germline tissue and decreased levels of WAGO-1 compared to wild-type worms (Fig. 3c, and Extended Data Fig. 4c, e). CSR-1 is known to bind histone mRNAs and is thought to participate in the 3' end cleavage of histone mRNAs<sup>38</sup> together with its interacting stem-loop binding protein CDL-1<sup>39</sup> (Fig. 4a, Extended Data Fig. 4d). Metaprofile analysis of histone 22G-RNAs in *piwi* mutant showed a strong bias towards the end of the histone genes (Extended Data Fig. 4f), right upstream to the location of the stem-loop structure bound by CDL-1 (Fig. 4c). Thus, in the absence of PIWI the histone mRNA 3' end cleavage by CSR-1 and CDL-1 may trigger the production of histone 22G-RNAs loaded into WAGO-1. To test this hypothesis, we mutated the catalytic domain of CSR-1 by CRISPR-Cas9 and crossed this strain with the *piwi* mutant. We observed a substantial reduction of histone 22G-RNAs in *piwi* mutant animals where the catalytic activity of CSR-1 was zygotically abolished (Fig. 4d). Similar results were obtained by using *csr-1* RNAi treatment in the *piwi* mutant (Extended Data Fig. 4g). Moreover, RNAi treatment of CDL-1 results in a slight reduction of 22G-RNAs in the region corresponding to the location of the stem-loop structure and spreading of 22G-RNAs along the

coding region towards the 5' end (Extended Data Fig. 4h). These results suggest that the interaction between CSR-1 and CDL-1 help to focus the cleavage activity of CSR-1 in proximity of the stem loop structure, and this triggers the synthesis and loading of histone 22G-RNAs into the WAGO pathway in absence of PIWI.

### **Inactivation of downstream components of the piRNA pathway restores histone expression and *piwi* mutant fertility**

To determine whether the histone 22G-RNAs cause the transgenerational loss of fertility in piRNA mutant worms, we set out to rescue the fertility defects by inactivating the downstream piRNA factors responsible for the production of 22G-RNAs. MUT-16 is one of the biogenesis factors that promote the synthesis of 22G-RNAs loaded into WAGOs<sup>40</sup> and interacts with PIWI (Fig. 2a). RNAi depletion of MUT-16 (Fig. 5a) over two generations restored *piwi* mutant fertility (Fig. 5b), and *piwi* mutant worms treated continuously with *mut-16* RNAi did not become sterile (Extended Data Fig. 5a, b). Additionally, *mut-16* RNAi treatment on sterile *piwi* mutant worms was sufficient to restore their fertility. RNAi depletion of WAGO-1 also restored the fertility of sterile *piwi* mutant worms (Fig. 5g). However, the restored fertility was lower than *mut-16* RNAi treatment, suggesting that other Argonaute proteins might participate in histone mRNA silencing in *piwi* mutant (Fig. 5g). Indeed, RNAi treatment of *ppw-1* or *ppw-2*, the two other Argonautes that interact with CSR-1, PIWI and WAGO-1 (Fig. 4a), showed rescued *piwi* mutant fertility (Extended Data Fig. 5 c, d). Instead, RNAi knock down of HRDE-1 did not recover *piwi* fertility, likely because histone mRNAs are mainly silenced at the post-transcriptional level (Extended Data Fig. 5c, d). To demonstrate that the recovered fertility in *mut-16* RNAi treated animals was specifically promoted by the desilencing of histone mRNAs we analyzed 22G-RNAs and mRNAs using RNA-seq. The reduction of histone 22G-RNAs correlated with increased expression of the replicative

histone mRNAs in *mut-16* RNAi treated animals (Fig 5c, d). Five piRNA-dependent targets showed a modest re-silencing signature, suggesting that they were unlikely to contribute to the recovered fertility (Extended Data Fig. 5e). Absence of re-silencing of REs was observed upon *mut-16* RNAi treatment in the *piwi* mutant background (Fig. 5e). The rescued fertility of piRNA mutants treated with *mut-16* RNAi was instead accompanied by further desilencing of REs (Fig. 5e and Extended Data Fig. 5f). In addition, WAGO-1 remained cytoplasmic in those fertile animals, suggesting no restoration of canonical WAGO-1 silencing complex in germ granules (Fig. 5f). Moreover, WAGO-1 and CSR-1 interaction persisted even in absence of histone 22G-RNAs (Extended Data Fig. 4e), indicating that this interaction is upstream of histone 22G-RNA synthesis. Collectively, these results suggest that the removal of histone 22G-RNAs upon *mut-16* RNAi treatment and not the re-silencing of REs restored the fertility of *piwi* mutants.

### **Inheritance of *piwi* mutant phenotype and histone 22G-RNAs in wild-type worms**

To test whether inheritance of histone 22G-RNAs is sufficient to transmit a *piwi*-like phenotype in wild-type worms, we outcrossed *prg-1(n4357)* hermaphrodites with wild-type males (Fig. 6a). We used worms from later generations of the *prg-1* mutants, which were almost completely sterile, to select individuals expressing high levels of histone 22G-RNAs (Fig. 6b). In 2 out of 5 crosses we selected three heterozygotes (+/-) F1 lines in each cross, and propagated two F2 homozygote (-/-) *prg-1(n4357)* mutant and one wild-type (+/+) animals from each line and analyzed the brood of the F3 progeny (Fig. 6b and Extended Data Fig. 6a-d). The homozygote *prg-1(n4357)* mutants remained almost completely sterile after the cross (Fig. 6b, and Extended Data Fig. 6a, c). The homozygote wild-type (+/+) animals displayed a *piwi*-like phenotype, showing reduced fertility compared to the parental P0 wild-type (Fig. 6b, and Extended Data Fig. 6a, c). To determine whether this reduced fertility was caused by inherited DNA mutations, we performed

brood size assay on all the progeny from one of the most affected F3 worms. All the resulting F4 animals showed increased fertility compared to the parental F3 animal (Fig. 6c), indicating that DNA mutation was not responsible for the observed phenotype in outcrossed wild-type worms. To further exclude possible genetic effects of the parental *prg-1(n4357)* mutant allele, we repeated the outcross experiment using one of the *prg-1* mutant allele generated by CRISPR-Cas9 (Extended Data Fig. 6g), and observed the same results (Fig. 6d and Extended Data Fig. 6e, f). In addition, we propagated the selected outcrossed homozygote wild-type lines for three subsequent generations and observed a gradual recovery of fertility (Fig. 6d), even though some wild-type lines did not completely recover the parental level of fertility. Sequencing 22G-RNAs from three of the outcrossed homozygote wild-type lines after 6 generations revealed inherited histone 22G-RNAs (Fig. 6e). We also crossed heterozygote hermaphrodite animals with wild-type males, and we observed similar inherited phenotype in wild-type worms (Fig. 6f, g and Extended Data Fig. 6h, i). Based on these results, we propose that the maternal transmission of a pool of histone 22G-RNAs into wild-type worms can epigenetically affects their fertility.

## Discussion

Here we have revealed the epigenetic mechanism underlying the transgenerational loss of fertility in *C. elegans* piRNA mutants. We have shown that the *piwi* phenotype is not related to the role of piRNAs in repressing REs, but results from the inheritance of a pool of 22G-RNAs that are antisense to histone mRNAs, leading to the post-transcriptional silencing of all the replicative histone genes. Previous reports have proposed that the sterility of *piwi* mutants is a consequence of “heritable stress” caused by REs derepression, which lead to a form of adult diapause in late generations of *piwi* mutant<sup>6,41</sup>. Our RNA-seq analysis of almost 60,000 individual REs has shown that only less than 100 REs are upregulated in *piwi* mutant across generations, and their

upregulation does not correlate with the sterility phenotype. Instead, we have documented the transgenerational silencing of histone mRNAs by 22G-RNAs, which causes a reduction in the pool of histone proteins and lack of incorporation of histones into the chromatin. The lack of histone incorporation into chromatin and defects in chromosome compaction can explain the reported cell death and germ cell atrophy in sterile *piwi* mutant animals<sup>41</sup>. Thus, we propose that the inheritance of histone 22G-RNAs underlie the “heritable stress” that ultimately lead to sterile animals.

Our results show that the silencing of histone genes is caused by targeting of the WAGO pathway away from piRNA-dependent 22G-RNA targets to histone mRNAs. This process requires several worm generations, possibly because the WAGO pathway can still be recruited to piRNA-dependent 22G-RNA targets in the absence of PIWI for several generations. We speculate that the germ granule localization of WAGO-1 and its interaction with specific germ granule components, such as DEPS-1, help to maintain the piRNA-induced WAGO-1 silencing complex on piRNA targets even in absence of PIWI for certain generations. However, the interaction between WAGO-1 and DEPS-1 might not be stable without PIWI, and WAGO-1 interaction with CSR-1 might be favored in the cytoplasm allowing WAGO-1 silencing complex to localize on histone mRNAs. In support of this hypothesis, we have shown that WAGO-1 interaction with germ granule components is gradually decreased across generations of *piwi* mutant, even though it is still capable of interacting in the cytoplasm with the 22G-RNA biogenesis factor RDE-12 and the Argonaute CSR-1. In addition to WAGO-1, other downstream Argonautes of the piRNA pathway might relocalize on histone mRNAs in absence of PIWI. We have shown that two of these Argonaute, PPW-1 and PPW-2, which also interacts with CSR-1 in wild-type worms, are required for histone mRNA silencing in *piwi* mutant, suggesting they might also relocalize on histone mRNAs similarly to WAGO-1.

Our results suggest that the cleavage of histone pre-mRNAs by CSR-1 is required to facilitate the synthesis and loading of histone 22G-RNAs by the WAGO pathway in absence of PIWI. CSR-1 may also cleave other germline mRNA targets<sup>42</sup>. However, we did not observe silencing of CSR-1 mRNA targets by the WAGO pathway in *prg-1* mutants. One possibility is that the amount of cleavage product from CSR-1 mRNA targets is much lower than the cleaved histone mRNAs. Alternatively, other factors, such as mRNA-specific nucleotide sequences<sup>18,43</sup>, may prevent germline mRNAs from becoming targets of the WAGO pathway in the absence of piRNAs.

Our results, together with previous reports<sup>28,29</sup>, suggest that piRNAs might only be required to initiate and not to maintain the silencing of REs. Nonetheless, a continuous synthesis of piRNAs is required in each generation to repress potential RE invasions. We speculate that the piRNA-driven production of WAGO-bound 22G-RNAs we observed against more than a thousand of protein-coding genes functions to maintain the piRNA-induced silencing complex in readiness to silence foreign RNAs. Nonetheless, it is unclear how the piRNA pathway can be evolutionary retained if it is only “waiting” for a potential invasion. Previous works have shown the physiological function of PIWI in regulating some germline mRNA targets<sup>44,45</sup>. Based on our results, we propose a model where the coupling between the lack of piRNAs and the consequent silencing of histone genes, initiated by CSR-1 and CDL-1, acts as the evolutionary force that maintains a functional piRNA-induced silencing pathway (Extended Data Fig. 7). Thus, the processing of histone mRNAs by CSR-1 and the co-evolution and co-existence of both the piRNA and the CSR-1 pathways could be an important evolutionary force in keeping the piRNA pathway in some nematode lineages. Indeed, nematode clades that have lost the piRNA pathway also lack CSR-1<sup>46</sup>, except for clade III nematodes<sup>47</sup>, which retain the CSR-1 pathway. We speculate that clade III nematodes escaped the sterility phenotype because they have polyadenylated histone mRNAs<sup>48</sup>, which likely do not require CSR-1 and CDL-1 for their processing.

We have observed the transmission of a *piwi*-like phenotype in wild-type worms through small RNAs. These results implicate small RNAs as molecules capable of transmitting epigenetic information between individuals and across generations, over and above the information encoded in their genomes.

## **ACKNOWLEDGEMENTS**

We thank the members of the Cecere laboratory, Daniele Canzio, Nicola Iovino, Ritwick Sawarkar and Peter Andersen for helpful discussions on the manuscript. We thank the Miska, the Mello, the Kennedy, the Seydoux, the Claycomb, the Strome, and the Dumont laboratories for sharing strains and/or antibodies. Some strains were provided by the CGC, funded by NIH Office of Research Infrastructure Programs (P40 OD010440). This project has received funding from the Institut Pasteur, the CNRS, and the European Research Council (ERC) under the European Union's Horizon 2020 research and innovation programme under grant agreement No ERC-StG- 679243. G.B. is part of the Pasteur - Paris University (PPU) International PhD Program and has received funding from the European Union's Horizon 2020 research and innovation programme under the Marie Skłodowska-Curie grant agreement No 665807. E.C. was supported by a Pasteur-Cantarini Fellowship program. F.D. and D.L. has received funding from “Région Ile-de-France” and Fondation pour la Recherche Médicale grants to support this study.

## **AUTHOR CONTRIBUTIONS**

G.C. identified and developed the core questions addressed in the project and analyzed the results of all experiments. G.B. performed most of the experiments and helped in the analysis of the results. E.C. Conceived and generated all the CRISPR-Cas9 lines used in this study, designed and performed the experiment using catalytic mutant of CSR-1, and performed all the confocal live imaging experiments. M.S. performed all the Co-immunoprecipitation and immunoprecipitation

experiments for mass spectrometry and Co-IPs. F.D. and D.L. performed the mass spectrometry and analyzed the data together with M.S. and G.C. B.L. performed the bioinformatic analysis of all the sequencing data. M.U. performed some RNA extraction and the RT-qPCR experiment. A.S. performed the brood size of the RNAi experiments under the supervision of G.B. C.D. performed the brood size of some RNAi and crossing experiments together with G.C. P.Q. performed the GRO-seq. E.C. and P.Q. contributed to collect some RNA samples used for the initial RNA-seq experiments. G.C. wrote the paper with the contribution of G.B., E.C., M.S., B.L.

**COMPETING INTERESTS:** All the authors declare no competing interests.

## REFERENCES

1. Ozata, D. M., Gainetdinov, I., Zoch, A., O'Carroll, D. & Zamore, P. D. PIWI-interacting RNAs: small RNAs with big functions. *Nature Reviews Genetics* (2019).  
doi:10.1038/s41576-018-0073-3
2. Thomson, T. & Lin, H. The Biogenesis and Function of PIWI Proteins and piRNAs: Progress and Prospect. *Annu. Rev. Cell Dev. Biol.* (2009).  
doi:10.1146/annurev.cellbio.24.110707.175327
3. Tóth, K. F., Pezic, D., Stuwe, E. & Webster, A. The pirna pathway guards the germline genome against transposable elements. in *Advances in Experimental Medicine and Biology* (2016). doi:10.1007/978-94-017-7417-8\_4
4. Wu, P.-H. *et al.* An Evolutionarily Conserved piRNA-producing Locus Required for Male Mouse Fertility. *bioRxiv* 386201 (2018). doi:10.1101/386201
5. Gou, L. T. *et al.* Ubiquitination-Deficient Mutations in Human Piwi Cause Male Infertility by Impairing Histone-to-Protamine Exchange during Spermiogenesis. *Cell* (2017).  
doi:10.1016/j.cell.2017.04.034

6. Simon, M. *et al.* Reduced Insulin/IGF-1 Signaling Restores Germ Cell Immortality to *Caenorhabditis elegans* Piwi Mutants. *Cell Rep.* (2014). doi:10.1016/j.celrep.2014.03.056
7. Katz, D. J., Edwards, T. M., Reinke, V. & Kelly, W. G. A *C. elegans* LSD1 Demethylase Contributes to Germline Immortality by Reprogramming Epigenetic Memory. *Cell* (2009). doi:10.1016/j.cell.2009.02.015
8. Buckley, B. A. *et al.* A nuclear Argonaute promotes multigenerational epigenetic inheritance and germline immortality. *Nature* (2012). doi:10.1038/nature11352
9. Frézal, L., Demoinet, E., Braendle, C., Miska, E. & Félix, M.-A. Natural Genetic Variation in a Multigenerational Phenotype in *C. elegans*. *Curr. Biol.* **28**, 2588-2596.e8 (2018).
10. Spracklin, G. *et al.* Identification and Characterization of *C. elegans* RNAi Inheritance Machinery. *Genetics* 1–19 (2017). doi:10.20944/preprints201702.0096.v1
11. Perez, M. F. & Lehner, B. Intergenerational and transgenerational epigenetic inheritance in animals. *Nat. Cell Biol.* **21**, 143–151 (2019).
12. Batista, P. J. *et al.* PRG-1 and 21U-RNAs Interact to Form the piRNA Complex Required for Fertility in *C. elegans*. *Mol. Cell* (2008). doi:10.1016/j.molcel.2008.06.002
13. Ruby, J. G. *et al.* Large-Scale Sequencing Reveals 21U-RNAs and Additional MicroRNAs and Endogenous siRNAs in *C. elegans*. *Cell* (2006). doi:10.1016/j.cell.2006.10.040
14. Das, P. P. *et al.* Piwi and piRNAs Act Upstream of an Endogenous siRNA Pathway to Suppress Tc3 Transposon Mobility in the *Caenorhabditis elegans* Germline. *Mol. Cell* (2008). doi:10.1016/j.molcel.2008.06.003
15. Cecere, G., Zheng, G. X. Y., Mansisidor, A. R., Klymko, K. E. & Grishok, A. Promoters Recognized by Forkhead Proteins Exist for Individual 21U-RNAs. *Mol. Cell* **47**, 734–745 (2012).
16. Gu, W. *et al.* CapSeq and CIP-TAP identify pol ii start sites and reveal capped small

- RNAs as *C. elegans* piRNA precursors. *Cell* (2012). doi:10.1016/j.cell.2012.11.023
17. Shen, E. Z. *et al.* Identification of piRNA Binding Sites Reveals the Argonaute Regulatory Landscape of the *C. elegans* Germline. *Cell* (2018). doi:10.1016/j.cell.2018.02.002
  18. Zhang, D. *et al.* The piRNA targeting rules and the resistance to piRNA silencing in endogenous genes. *Science* (80-. ). (2018). doi:10.1126/science.aao2840
  19. Lee, H. C. *et al.* *C. elegans* piRNAs mediate the genome-wide surveillance of germline transcripts. *Cell* (2012). doi:10.1016/j.cell.2012.06.016
  20. Bagijn, M. P. *et al.* Function, targets, and evolution of *Caenorhabditis elegans* piRNAs. *Science* (80-. ). (2012). doi:10.1126/science.1220952
  21. Hourri-Ze'evi, L. *et al.* A Tunable Mechanism Determines the Duration of the Transgenerational Small RNA Inheritance in *C. elegans*. *Cell* (2016). doi:10.1016/j.cell.2016.02.057
  22. Spracklin, G. *et al.* The RNAi inheritance machinery of *caenorhabditis elegans*. *Genetics* (2017). doi:10.1534/genetics.116.198812
  23. Wan, G. *et al.* Spatiotemporal regulation of liquid-like condensates in epigenetic inheritance. *Nature* (2018). doi:10.1038/s41586-018-0132-0
  24. Zeller, P. *et al.* Histone H3K9 methylation is dispensable for *Caenorhabditis elegans* development but suppresses RNA:DNA hybrid-associated repeat instability. *Nat. Genet.* (2016). doi:10.1038/ng.3672
  25. McMurchy, A. N. *et al.* A team of heterochromatin factors collaborates with small RNA pathways to combat repetitive elements and germline stress. *Elife* (2017). doi:10.7554/eLife.21666
  26. Ni, J. Z., Chen, E. & Gu, S. G. Complex coding of endogenous siRNA, transcriptional silencing and H3K9 methylation on native targets of germline nuclear RNAi in *C. elegans*.

- BMC Genomics* (2014). doi:10.1186/1471-2164-15-1157
27. Shirayama, M. *et al.* PiRNAs initiate an epigenetic memory of nonself RNA in the *C. elegans* germline. *Cell* (2012). doi:10.1016/j.cell.2012.06.015
  28. de Albuquerque, B. F. M., Placentino, M. & Ketting, R. F. Maternal piRNAs Are Essential for Germline Development following De Novo Establishment of Endo-siRNAs in *Caenorhabditis elegans*. *Dev. Cell* (2015). doi:10.1016/j.devcel.2015.07.010
  29. Phillips, C. M., Brown, K. C., Montgomery, B. E., Ruvkun, G. & Montgomery, T. A. PiRNAs and piRNA-Dependent siRNAs Protect Conserved and Essential *C. elegans* Genes from Misrouting into the RNAi Pathway. *Dev. Cell* (2015). doi:10.1016/j.devcel.2015.07.009
  30. Weick, E. M. *et al.* PRDE-1 is a nuclear factor essential for the biogenesis of Ruby motif-dependent piRNAs in *C. elegans*. *Genes Dev.* (2014). doi:10.1101/gad.238105.114
  31. Pettitt, J., Crombie, C., Schümperli, D. & Müller, B. The *Caenorhabditis elegans* histone hairpin-binding protein is required for core histone gene expression and is essential for embryonic and postembryonic cell division. *J. Cell Sci.* (2002).
  32. Kodama, Y., Rothman, J. H., Sugimoto, A. & Yamamoto, M. The stem-loop binding protein CDL-1 is required for chromosome condensation, progression of cell death and morphogenesis in *Caenorhabditis elegans*. *Development* (2002).
  33. Gu, W. *et al.* Distinct Argonaute-Mediated 22G-RNA Pathways Direct Genome Surveillance in the *C. elegans* Germline. *Mol. Cell* (2009). doi:10.1016/j.molcel.2009.09.020
  34. Spike, C. A., Bader, J., Reinke, V. & Strome, S. DEPS-1 promotes P-granule assembly and RNA interference in *C. elegans* germ cells. *Development* (2008). doi:10.1242/dev.015552
  35. Shirayama, M., Stanney, W., Gu, W., Seth, M. & Mello, C. C. The Vasa homolog RDE-12

engages target mRNA and multiple argonaute proteins to promote RNAi in *C. elegans*.

*Curr. Biol.* (2014). doi:10.1016/j.cub.2014.03.008

36. Wedeles, C. J., Wu, M. Z. & Claycomb, J. M. Protection of germline gene expression by the *C. elegans* argonaute CSR-1. *Dev. Cell* (2013). doi:10.1016/j.devcel.2013.11.016
37. Seth, M. *et al.* The *C. elegans* CSR-1 argonaute pathway counteracts epigenetic silencing to promote germline gene expression. *Dev. Cell* (2013). doi:10.1016/j.devcel.2013.11.014
38. Avgousti, D. C., Palani, S., Sherman, Y. & Grishok, A. CSR-1 RNAi pathway positively regulates histone expression in *C. elegans*. *EMBO J.* (2012). doi:10.1038/emboj.2012.216
39. Keall, R., Whitelaw, S., Pettitt, J. & Müller, B. Histone gene expression and histone mRNA 3' end structure in *Caenorhabditis elegans*. *BMC Mol. Biol.* (2007). doi:10.1186/1471-2199-8-51
40. Zhang, C. *et al.* mut-16 and other mutator class genes modulate 22G and 26G siRNA pathways in *Caenorhabditis elegans*. *Proc. Natl. Acad. Sci.* (2011). doi:10.1073/pnas.1018695108
41. Heestand, B., Simon, M., Frenk, S., Titov, D. & Ahmed, S. Transgenerational Sterility of Piwi Mutants Represents a Dynamic Form of Adult Reproductive Diapause. *Cell Rep.* (2018). doi:10.1016/j.celrep.2018.03.015
42. Gerson-Gurwitz, A. *et al.* A Small RNA-Catalytic Argonaute Pathway Tunes Germline Transcript Levels to Ensure Embryonic Divisions. *Cell* (2016). doi:10.1016/j.cell.2016.02.040
43. Seth, M. *et al.* The Coding Regions of Germline mRNAs Confer Sensitivity to Argonaute Regulation in *C. elegans*. *Cell Rep.* (2018). doi:10.1016/j.celrep.2018.02.009
44. Tang, W. *et al.* A Sex Chromosome piRNA Promotes Robust Dosage Compensation and Sex Determination in *C. elegans*. *Dev. Cell* (2018). doi:10.1016/j.devcel.2018.01.025

45. Barberán-Soler, S. *et al.* Co-option of the piRNA pathway for germline-specific alternative splicing of *C. elegans* TOR. *Cell Rep.* (2014). doi:10.1016/j.celrep.2014.08.016
46. Sarkies, P. *et al.* Ancient and Novel Small RNA Pathways Compensate for the Loss of piRNAs in Multiple Independent Nematode Lineages. *PLoS Biol.* (2015). doi:10.1371/journal.pbio.1002061
47. Tu, S. *et al.* Comparative functional characterization of the CSR-1 22G-RNA pathway in *Caenorhabditis* nematodes. *Nucleic Acids Res.* (2015). doi:10.1093/nar/gku1308
48. Wyler-Duda, P., Bernard, V., Stadler, M., Suter, D. & Schümperli, D. Histone H4 mRNA from the nematode *Ascaris lumbricoides* is cis-spliced and polyadenylated. *Biochim. Biophys. Acta - Gene Struct. Expr.* (1997). doi:10.1016/S0167-4781(96)00235-7

**Fig. 1**

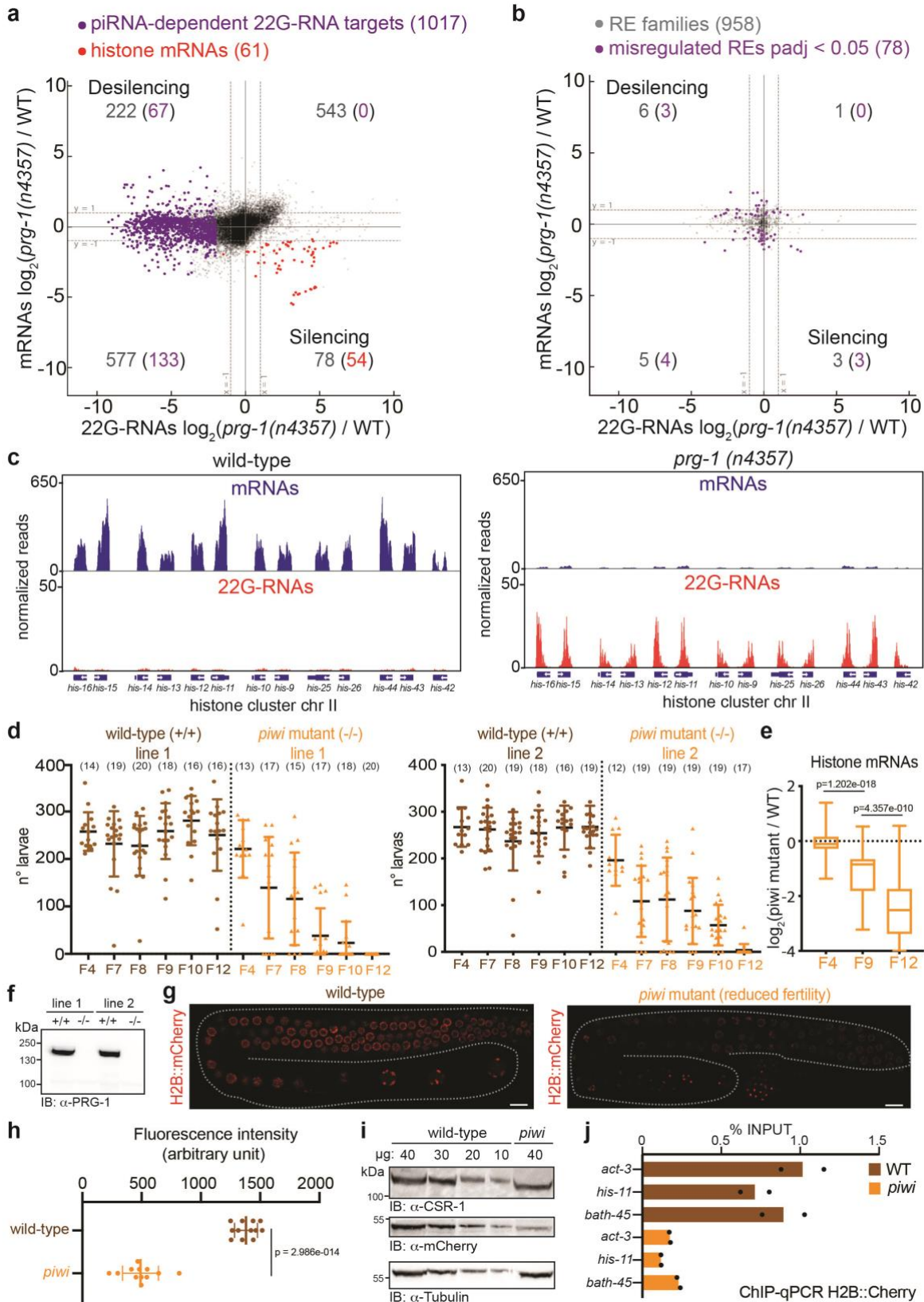


**Fig. 1: Histone mRNAs silencing by 22G-RNAs correlates with progressive sterility in *piwi* mutant**

**a**, Comparison between mRNA log<sub>2</sub> fold change (y axis) and 22G-RNA log<sub>2</sub> fold change (x axis) in *prg-1 (n4357)* mutant vs. wild-type worms for protein-coding genes. piRNA-dependent 22G-RNA targets (purple dots) and replicative histone genes (red dots) are indicated. The dashed lines indicate the two-fold changes, and the number in parenthesis indicates the portion of misregulated genes (two-fold changes, padj < 0.05) belonging to the piRNA-dependent 22G-RNA targets (purple) or histone genes (red). Wald test has been used by *deseq2* to calculate the p value. n = 18667. **b**, Same comparison as in **a** considering only RE families. Significant misregulated RE families are indicated (padj < 0.05, n=958). **c**, Genomic view of one histone gene cluster showing normalized RNA-seq reads for mRNAs (blue tracks) and 22G-RNAs (red tracks) in wild-type (left panel) and *prg-1(n4357)* mutant (right panel). **d**, Schematic of the transgenerational experiments using the CRISPR-Cas9 *piwi* mutant and wild-type lines. **e**, Brood size assay of the experiment described in **d**. Dots or rectangles correspond to the total number of alive larvae from individual worms. The black lines indicate the mean, the error bars the standard deviation, and the sample size (n) is indicated in parenthesis. **f**, Box plots showing multiple generations log<sub>2</sub> fold change of histone mRNAs in CRISPR-Cas9 *piwi* mutant compared to wild-type. Box plots display median (line), first and third quartiles (box) and highest/lowest value (whiskers). Two-tailed p value calculated using Mann-Whitney-Wilcoxon tests is shown. **g**, On the right, representative images of germline-expressed H2B::mCherry in wild-type and *piwi* mutant worms. White bars indicate 10μM size. On the left, H2B::mCherry quantification using the mean intensity of 15 pachytene nuclei in each individual worm analysed. The mean and standard deviation is shown. \*\*\*\*\*: two-tailed p value <0.0001; Unpaired t test. n=12 **h**, H2B::mCherry chromatin immunoprecipitation (ChIP) in wild-type and *piwi* mutant. The amount of immunoprecipitated DNA is shown as percentage of

input DNA. The bars indicate the mean and the black dots individual data. n=2 biologically independent experiments. Data available in Source Data Fig. 1.

**Fig. 2**

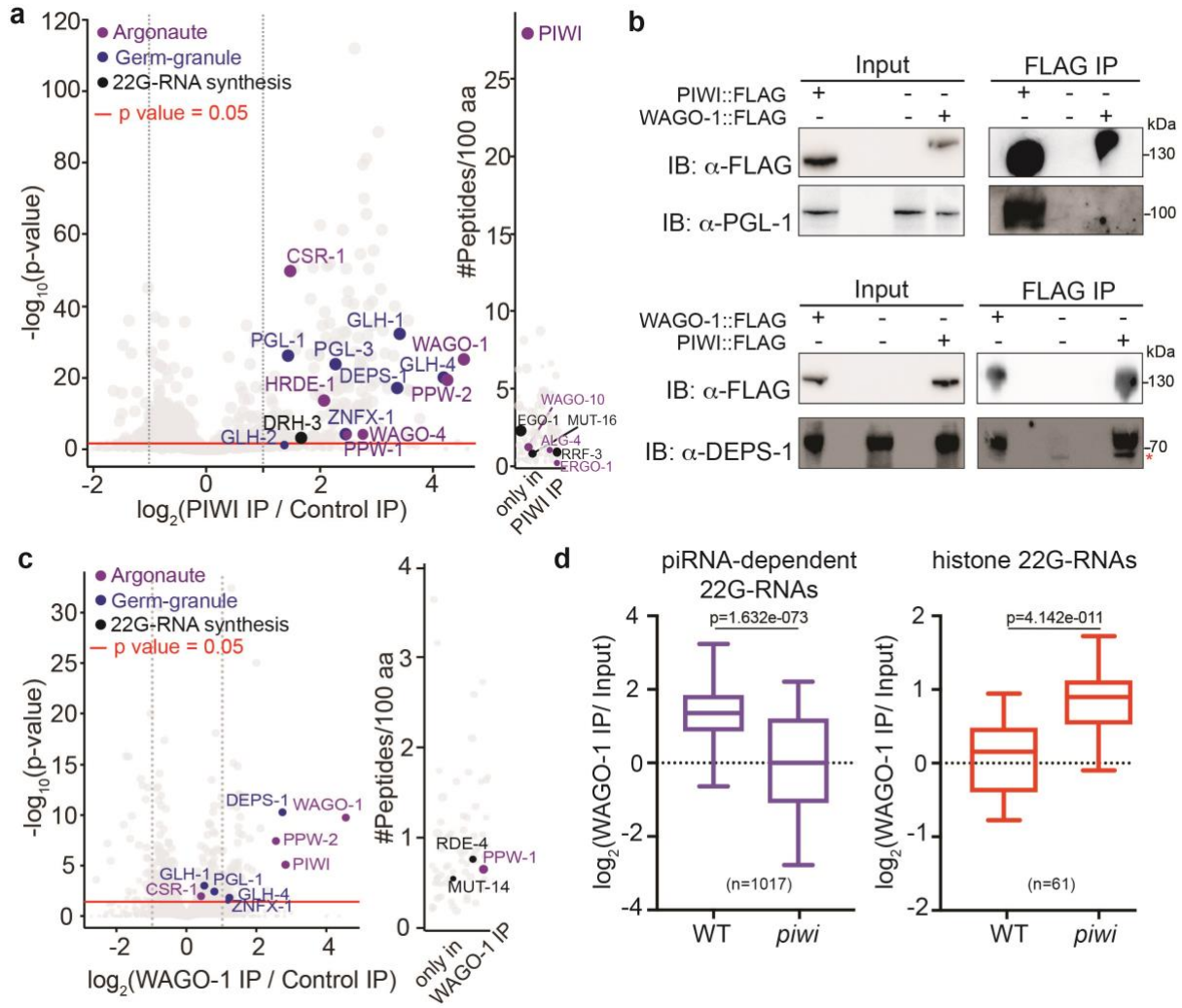


**Fig. 2: Loading of histone 22G-RNAs into WAGO-1 upon disruption of the piRNA-induced silencing complex**

**a**, Volcano plot showing enrichment values and corresponding significance levels for proteins co-purifying with PIWI (see also Supplementary Table 1). Argonaute proteins, germ granule components and 22G-RNA biogenesis factors are labelled with different colours. The size of the dots is proportional to the number of peptides used for the quantification. The linear model was used to compute protein quantification ratio and the red horizontal line indicates the two-tailed p value = 0.05. n=4 biologically independent experiments. **b**, Co-IP experiments showing DEPS-1 interactions with PIWI and WAGO-1 and PGL-1 interaction with PIWI and not with WAGO-1.

Presence (+) or absence (-) of the tagged proteins are indicated. Immunoprecipitation was performed using  $\alpha$ -FLAG antibody, and the blots were probed with  $\alpha$ -PGL-1,  $\alpha$ -DEPS-1 or  $\alpha$ -FLAG antibodies. \* the lower band signal corresponds to a non-specific protein. The experiment was repeated twice. **c**, Volcano plots showing  $\log_2$  fold change and corresponding significance levels of proteins co-purifying with WAGO-1 in wild-type worm lysate as in **a**. Argonaute proteins, germ granule components and 22G-RNA biogenesis factors are labelled with different colours. The size of the dots is proportional to the number of peptides used for the quantification. The linear model was used to compute protein quantification ratio and the red horizontal line indicates the two-tailed p value = 0.05. n=4 biologically independent experiments. **d**, Box plots showing the  $\log_2$  fold change of the ratio between piRNA-dependent 22G-RNA and histone 22G-RNA normalized reads from WAGO-1 immunoprecipitation (IP) and total RNA (Input) in wild-type and *piwi* mutant background. Box plots display median (line), first and third quartiles (box) and the whiskers are drawn down to the 5th percentile and up to the 95th. Two-tailed p value calculated using Mann-Whitney-Wilcoxon tests is shown. Sample size (n) is shown in parenthesis. Data available in Source Data Fig. 2.

**Fig. 3**

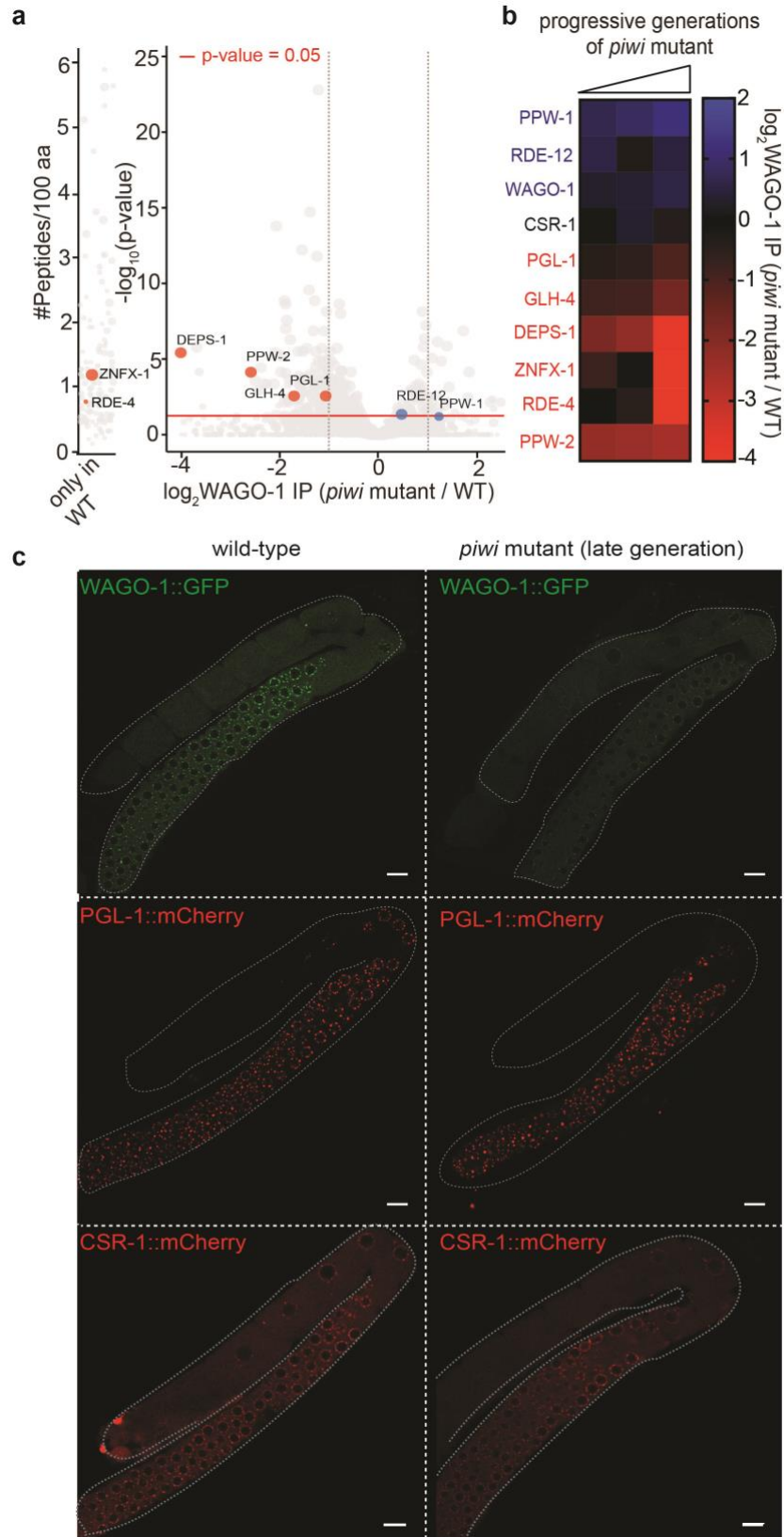


**Fig. 3: WAGO-1 loses interactions with germ granule components across generation of *piwi* mutant and remain cytoplasmic**

**a**, Volcano plots showing log<sub>2</sub> fold change and corresponding significance levels of proteins co-purifying with WAGO-1 in *piwi* mutant compared to wild-type. Significant decreased or increased interactions with WAGO-1-interacting germ granule components, Argonaute proteins or RNAi factor are shown in red and blue respectively. The size of the dots is proportional to the number of peptides used for the quantification. The linear model was used to compute protein quantification ratio and the red horizontal line indicates the two-tailed p value = 0.05. n=4 biologically independent experiments. **b**, Heatmap showing log<sub>2</sub> fold change of proteins co-purifying with WAGO-1 in *piwi* mutant at different generations compared to wild-type. Decreased or increased interactions with WAGO-1-interacting germ granule components, Argonaute proteins or RNAi factor are shown in red and blue respectively. n=4 biologically independent experiments. **c**, Live confocal images of WAGO-1::GFP, PGL-1::mCherry, and CSR-1::mCherry showing loss of WAGO-1 germ granule localization in affected *piwi* mutant germlines compared to wild-type. The white bars indicate 10μM size. The experiment was repeated independently three times with similar results. Data available in Source Data Fig. 3.

**Fig. 4**

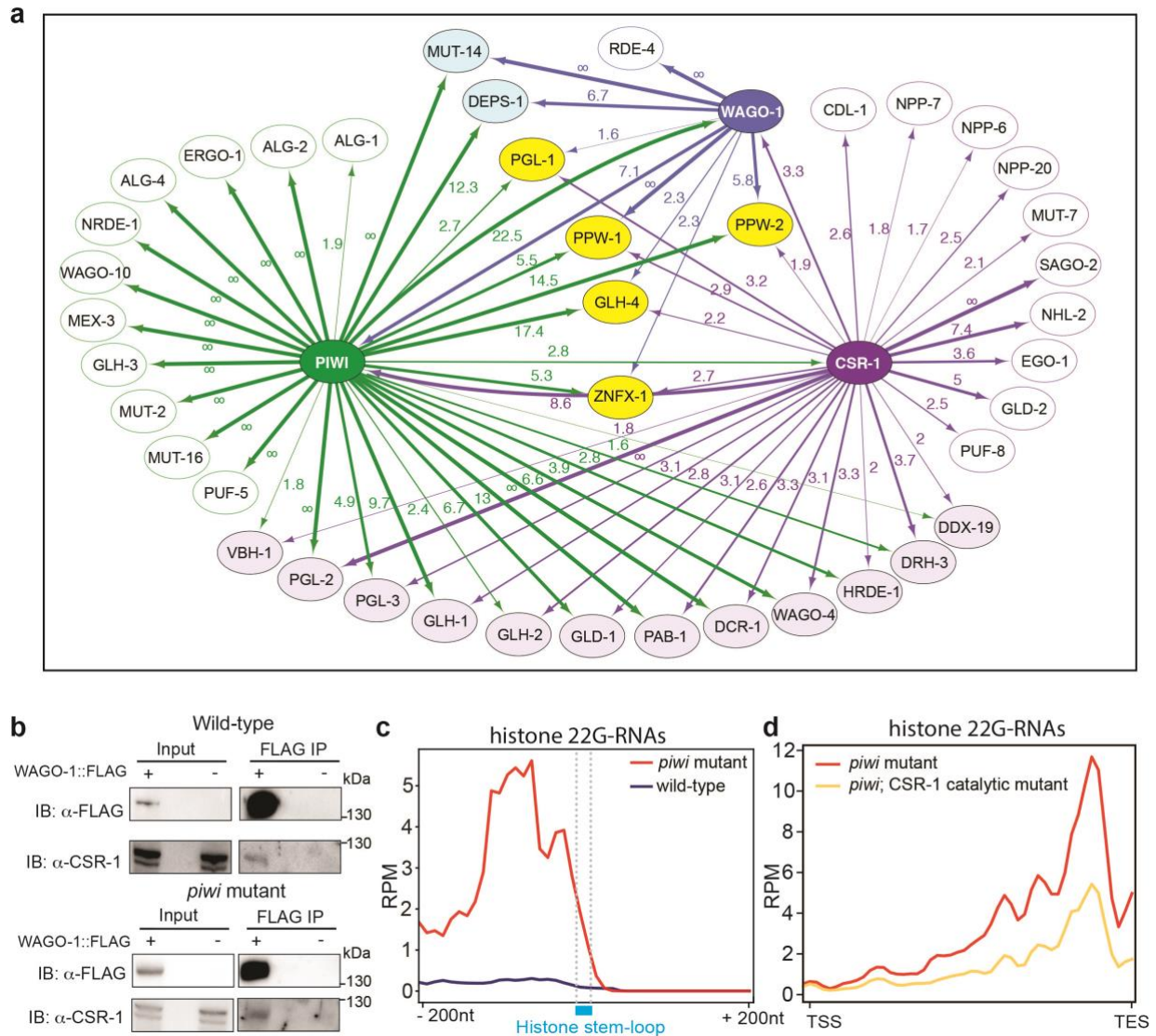


**Fig. 4: The CSR-1 pathway triggers the biogenesis of histone 22G-RNAs in *piwi* mutant**

**a**, Network interactome map showing the overlap between CSR-1, PIWI, and WAGO-1 interacting proteins by mass spec. Only a selection of interacting proteins is shown, corresponding to known germ granule components, RNAi factors and Argonaute proteins. Proteins interacting with CSR-1, PIWI and CSR-1 are shown in yellow. Proteins interacting only with PIWI and WAGO are shown in blue. Protein interacting only with CSR-1 and PIWI are shown in light violet. Numbers correspond to enrichment values in IPs and  $\infty$  represents proteins with their peptides detected

exclusively in the IP and not in the control. **b**, Co-IP experiments in wild-type (top) and *piwi* mutant (bottom) showing WAGO-1 interactions with CSR-1. Presence (+) or absence (-) of the tagged proteins are indicated. Immunoprecipitation was performed using  $\alpha$ -FLAG antibody, and the blots were probed with  $\alpha$ -CSR-1 or  $\alpha$ -FLAG antibodies. The amount of protein extract for immunoprecipitation was normalized on the total level of CSR-1 protein because mutant animals have less germline tissue (see also Extended Data Fig. 4e). The experiment was repeated independently two times with similar results. **c**, Metaprofile analysis showing the distribution of normalized 22G-RNA reads (RPM) 200nt upstream and 200nt downstream of the stem-loop sequence of histone mRNAs. The experiment was repeated independently two times with similar results. **d**, Metaprofile analysis showing the distribution of normalized 22G-RNA reads (RPM) across histone genes in *piwi* mutant background with (yellow line) or without (red line) mutation in the catalytic domain of CSR-1. TSS indicates the transcriptional start site, TES indicates the transcriptional end site. The experiment was repeated independently two times with similar results. Data available in Source Data Fig. 4.

**Fig. 5**

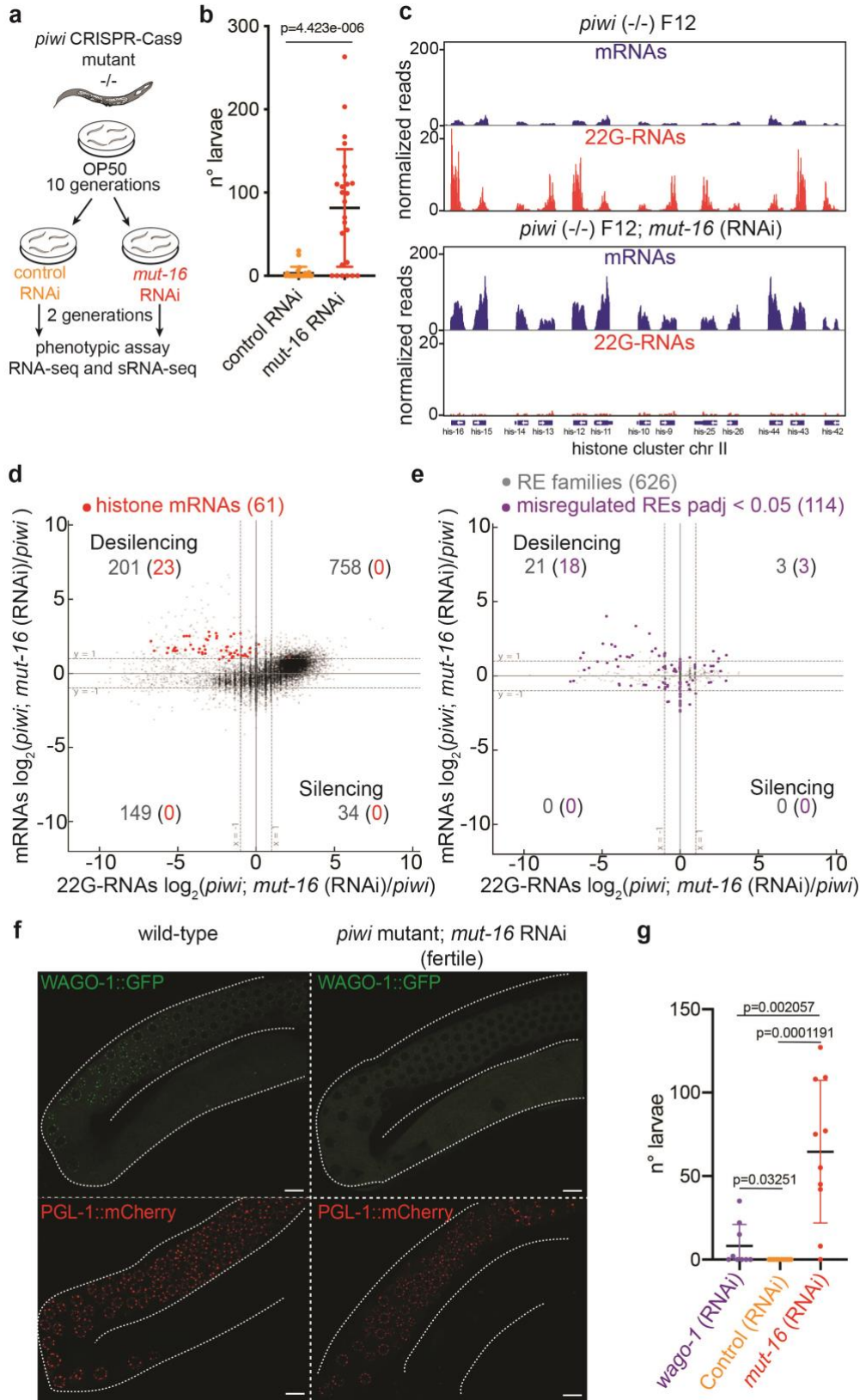


**Fig. 5: Removal of histone 22G-RNAs rescues *piwi* mutant transgenerational sterility**

**a**, Schematic of the RNAi experiment using CRISPR-Cas9 *piwi* mutant worms grown for 10 generations on plates seeded with *E. coli* OP50 and then shifted for two generations on plates seeded with *E. coli* expressing dsRNA targeting *mut-16* or empty vector. **b**, Results from brood size assay of the experiment described in **a**. Each dot corresponds to the total number of alive larvae from an individual worm. The black lines indicate the average brood size and the error bars the standard deviation. Two-tailed p value calculated using Mann-Whitney-Wilcoxon tests is shown. n= 25 **c**, Genomic view similar to **Fig. 1c** of one histone cluster in *piwi* mutant F12 treated with *mut-16* RNAi (lower panel) compared with *piwi* mutant F12 (upper panel). **d**, Comparison between mRNA log<sub>2</sub> fold change (y axis) and 22G-RNA log<sub>2</sub> fold change (x axis) in *piwi* mutant F12 treated with *mut-16* RNAi vs. *piwi* mutant F12 similar to **Fig. 1a**. Red dots indicate all the replicative histone genes. Wald test has been used by *deseq2* to calculate the p value. n = 18667 **e**, Same comparison as in **d**, except that families of REs were analysed. The purple dots indicate significantly misregulated RE families by RNA-seq (padj < 0.05). Wald test has been used by *deseq2* to calculate the p value. n = 626 **f**, Live confocal images of WAGO-1::GFP and PGL-1::mCherry showing lack of WAGO-1 germ granule localization in fertile *piwi* mutant upon *mut-16* RNAi treatment compared to wild-type. The white bars indicate 10µM size. The experiment was repeated independently three times with similar results. **g**, Results from brood size assay similar to the experiment described in **a**, except that sterile *piwi* mutant worms were used for the assay. Each dot corresponds to the total number of alive larvae from an individual worm. The black lines indicate the average brood size and the error bars the standard deviation. Two-tailed p value calculated using Mann-Whitney-Wilcoxon tests is shown. n = 10 Data available in Source Data Fig. 5.

## Fig. 6

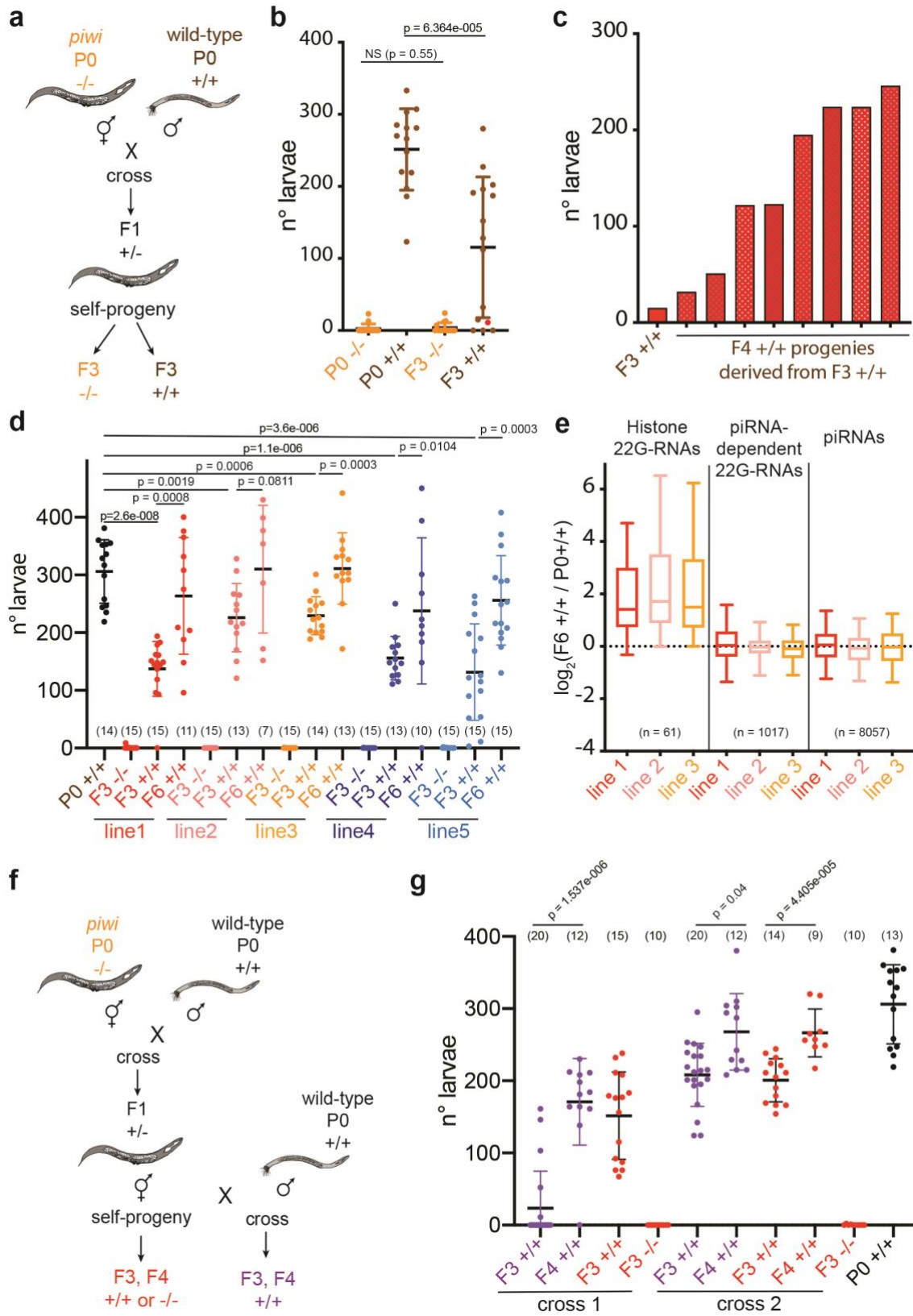


**Fig. 6: Histone 22G-RNAs facilitate the epigenetic inheritance of a *piwi*-like phenotype in wild-type worms**

**a**, Schematic of outcross between wild-type males (+/+) and hermaphrodite *prg-1(4357)* mutant (-/-) that are almost sterile. **b**, Brood size assay of the outcross experiment described in **a**. Each dot corresponds to the number of alive larvae from an individual worm. The black lines indicate the mean and the error bars the standard deviation. Two-tailed p value calculated using the Mann-Whitney-Wilcoxon tests is shown. n = 15 **c**, Brood size assay as in **b**, showing the increased brood of all the individual F4 +/+ animals (red bars) derived from the same F3 +/+ parental worm (also shown in **b**, as red dot). **d**, Brood size assay as in **b** of the outcross experiment described in Extended Data Fig. 6g. Five independent F2 wild-type outcrossed lines (+/+) were selected and propagated. The black lines indicate the mean, the error bars the standard deviation, and the sample size (n) is indicated in parenthesis. Two-tailed p value calculated using the Mann-Whitney-Wilcoxon tests is shown. **e**, Box plots of small RNA log<sub>2</sub> fold change of the F6 +/+ outcrossed line1 (red), line2 (pink) and line3 (yellow) compared with the parental P0 +/+. 22G-RNAs antisense to histone mRNAs and piRNA-dependent mRNA targets, and piRNAs are shown. Box plots display median (line), first and third quartiles (box) and the whiskers are drawn down to the 5th percentile and up to the 95th. Sample size (n) is indicated in parenthesis. **f**, Schematic of outcross between wild-type males (+/+) and hermaphrodite heterozygote *piwi* mutant (+/-) (purple) or self-progeny (red). After the cross wild-type (+/+) lines or self-crossed wild-type (+/+) and *piwi* mutant (-/-) lines were selected. Wild-type (+/+) lines were propagated for 2 generations (F3-F4). **g**, Brood size assay as in **b** of the outcross experiment described in **f**. The black lines indicate the mean and the error bars the standard deviation. Two-tailed p value calculated using the Mann-Whitney-Wilcoxon tests is shown. Data available in Source Data Fig. 6.